Journal of Applied Polymer Science

Redox-active LBL Films via *In Situ* Template Polymerization of Hydroquinone

Jian He, Ying Guan, Yongjun Zhang
Key Laboratory of Functional Polymer Materials, Institute of Polymer Chemistry, College of Chemistry, Nankai University, Tianjin 300071, China
Correspondence to: Y. Guan (E-mail: yingguan@nankai.edu.cn) or Y. Zhang (E-mail: yongjunzhang@nankai.edu.cn)

ABSTRACT: New redox-active hydrogel thin films with poly(hydroquinone) (PHQ) as polymeric redox couple and chitosan hydrogel as matrix are synthesized. Single-component layer-by-layer films of chitosan are first fabricated in a uniform and reproducible manner, which is proved by UV and AFM studies. The chitosan films are then treated in acidic hydroquinone (HQ) solution to introduce PHQ. *In situ* generation of PHQ in the films is proved by UV and FTIR spectroscopy. PHQ formation also results in an increased film roughness and thickness. We confirmed that oxygen acts as oxidant and chitosan acts as template in the polymerization of HQ. Cyclic voltammogram of the film presents two oxidation peaks at 0.21 and 0.75 V and one reduction peak at −0.15 V(vs Ag/AgCl), indicating the film, which is originally not redox-active, becomes redox-active after the introduction of PHQ. The new redox-active films may find applications in amperometric biosensors. © 2013 Wiley Periodicals, Inc. J. Appl. Polym. Sci. 129: 3070–3076, 2013

KEYWORDS: films; electrochemistry; self-assembly

Received 18 November 2012; accepted 19 January 2013; published online 18 February 2013
DOI: 10.1002/app.39043

INTRODUCTION

Hydrogels containing redox couples are redox-active because they allow for the conduction of electrons by self-exchange of electrons or holes between the rapidly reduced and rapidly oxidized redox functions.[1] A lot of redox hydrogels have been synthesized either by tethering redox couples, such as quinoid functions,[2] ferrocene,[3] and $Os^{2+/3+}$,[4] onto the polymer network, or trapping polymeric redox couples, such as polyaniline[5] and polypyrrole,[6] in a hydrogel matrix. These materials have found wide applications, especially in amperometric biosensors[5,7] and biofuel cells.[8]

Recently we synthesized a new redox hydrogel using poly(hydroquinone) (PHQ) as polymeric redox couple and chitosan as matrix.[9] PHQ was synthesized *in situ* by the oxidative polymerization of hydroquinone (HQ) using oxygen as oxidant and chitosan as template. As PHQ is a unique redox polymer which can undergo direct two-electron oxidation and reduction,[10] and chitosan is an attractive biopolymer,[11] the new redox hydrogel is expected to find applications in biomedical areas. To exploit its potential applications especially in biosensing, the very first step is that the gels are engineered into thin films. Previously the gel was smeared onto the electrode surface to form a coating.[9] This method is quite simple, however, it is difficult to control the film thickness.

Here we fabricated redox-active PHQ/chitosan thin films using a method combined the so-called layer-by-layer (LBL) assembly and the template polymerization of HQ. (Scheme 1) In LBL assembly, thin films are fabricated by alternate deposition of two polymers with complementary functional groups, using various interactions, such as electrostatic interaction, hydrogen bonding and covalent bonding, as driving forces.[12–18] The resulting films can be considered as hydrogels, as they are crosslinked polymeric networks which can swell in water.[19–21] As a method to fabricate hydrogel thin films, LBL assembly has the advantages over other methods as it allows for creating conformal coatings on substrates of any shape, and controlling film thickness on a nanometer scale.[19]

To fabricate the redox-active film, single-component LBL film of chitosan was first fabricated via the glutaraldehyde-mediated assembly of chitosan. Redox-active PHQ was then introduced into the film by *in situ* polymerization of HQ using chitason as template.(Scheme 1) LBL films have previously been used as nanoreactor for the *in situ* synthesis of inorganic nanoparticles, including nanoparticles of metal,[22–26] semiconductor,[22,27] and metal oxides/hydroxides.[28] The catalytic[29] and antimicrobial properties[30,31] of the resultant composite films have been exploited. In contrast, *in situ* synthesis of organic functional components in LBL films are rarely reported. The only examples include the *in situ* polymerization of aniline,[32] pyrrole,[33] and

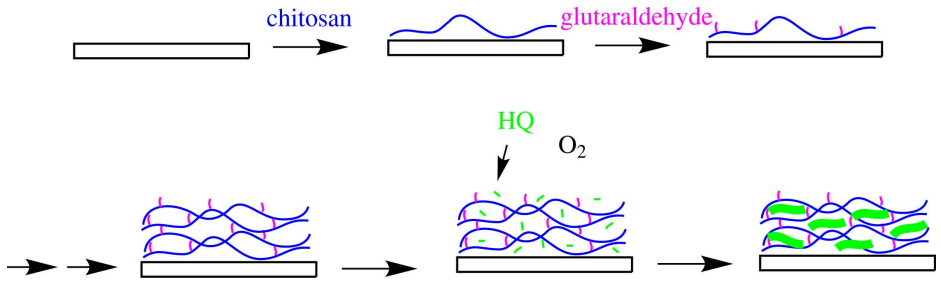

Scheme 1. Fabrication redox-active films of chitosan and PHQ. A single-component LBL film of chitosan was first fabricated via the glutaraldehyde-mediated assembly of chitosan. PHQ was then introduced by the *in situ* oxidative polymerization of HQ in the presence of oxygen using chitosan as template. [Color figure can be viewed in the online issue, which is available at wileyonlinelibrary.com.]

tyramine[34] in LBL multilayers. Usually the LBL films only serve as a confined place for the reactions to take place, in other words, the film materials do not participate in the reaction. The only exception may be the *in situ* polymerization of tyramine, which was catalyzed by an enzyme (horseradish peroxidase) embedded in the film.[34] Here the LBL film not only serves as nanoreactor, but also template for the polymerization of HQ.

EXPERIMENTAL

Materials

Chitosan with an M_v of 190,000–310,000 was obtained from Aldrich-Sigma. Polyethyleneimine (PEI) (M_w = 10,000) was purchased from Alfa Aesar. Hydroquinone (HQ), acetic acid (HAc), glutaraldehyde, and other chemicals are of analytical grade. Chitosan was purified according to Ref. 35. It was first dissolved in 0.1*M* HAc, and then precipitated with methanolic ammonia (70% methanol and 30% aqueous $NH_3 \cdot H_2O$). The solid obtained was washed four times with deionized water and three times with acetone, and dried at 40°C under reduced pressure.

Fabrication of Single-Component LBL Films of Chitosan or PEI

Single-component LBL films of chitosan were fabricated according to Ref. 36. Briefly, the substrates (quartz slides or silicon wafers) were first cleaned in boiling piranha solution (3 : 7 v/v H_2O_2–H_2SO_4 mixture) before use (Caution: this solution is extremely corrosive!). Films for electrochemical characterization were fabricated on ITO substrates which were cleaned according to a procedure described in Ref. 37. The substrates were placed in 0.5 wt % chitosan solution (in 0.1*M* HAc) for about 12 h for the deposition of the first layer of chitosan. The subsequent layers were deposited by alternate immersion in 2.5 wt % glutaraldehyde solution for 30 min and chitosan solution for 30 min, intermediated with 2 min water washing. Single-component LBL films of PEI were fabricated using the same procedure.

Oxidative Polymerization of Hydroquinone in the Chitosan LBL Films

To introduce PHQ, the chitosan films were simply immersed in 4.0 wt % HQ solution in 0.1*M* HAc. The solution was exposed to the air during the experiment. Temperature was controlled with a refrigerated circulator. After treated for a predetermined time, the films were withdrawn, cleaned thoroughly with water and air-dried.

Characterization

UV–vis absorption spectra were measured on a TU 1810PC UV–vis spectrophotometer (Purkinje General, China). Fourier transform infrared (FTIR) spectra were recorded on a Bio-Rad FTS-6000 spectrometer. Electrochemical characterization of the films was performed on a LK2005 electrochemical analysis system (Lanlike, China). Cyclic voltammetry (CV) measurements were performed in 0.01*M* phosphate buffer (pH = 7.3), using platinum and Ag/AgCl (saturated KCl) as the counter and reference electrode, respectively. The solutions were deoxygenated by bubbling nitrogen gas before the measurements.

RESULTS AND DISCUSSION

Synthesis and Characterization of the Single-Component Chitosan LBL Film

As shown in Scheme 1, to fabricate chitosan/PHQ thin film, the first step is the fabrication of single-component chitosan LBL film. Usually an LBL film is composed of at least two components. We[38] previously synthesized single-component chitosan LBL film by selective crosslinking chitosan in a chitosan/PAA (PAA: polyacrylic acid) film with glutaraldehyde, followed by the removal of PAA under alkali conditions. Recently Manna et al.[36] developed a more straightforward way, in which single-component chitosan LBL films were synthesized by glutaraldehyde-mediated assembly.

Here we adopted this method to fabricate single-component chitosan LBL films. The first layer of chitosan was deposited on the substrate via electrostatic interaction. By alternate dipping in glutaraldehyde and chitosan, subsequent layers of chitosan were assembled via the spontaneous covalent bonding between chitosan and glutaraldehyde (Scheme 2). The assembly process was followed by UV–vis spectroscopy. As shown in Figure 1, the absorption spectra of the films present two shoulders at ~225 and 265 nm, which can be assigned to the absorption of glutaraldehyde and chitosan, respectively, according to Manna et al.[36] A linear relationship between the film absorption and layer number was found, indicating that chitosan was assembled in a uniform and reproducible manner.

The morphology of the chitosan films was studied by AFM. As shown in Figure 2, a 10-layer film presents dome-like features with a size of ~350 nm. These features become less prominent

Applied Polymer SCIENCE

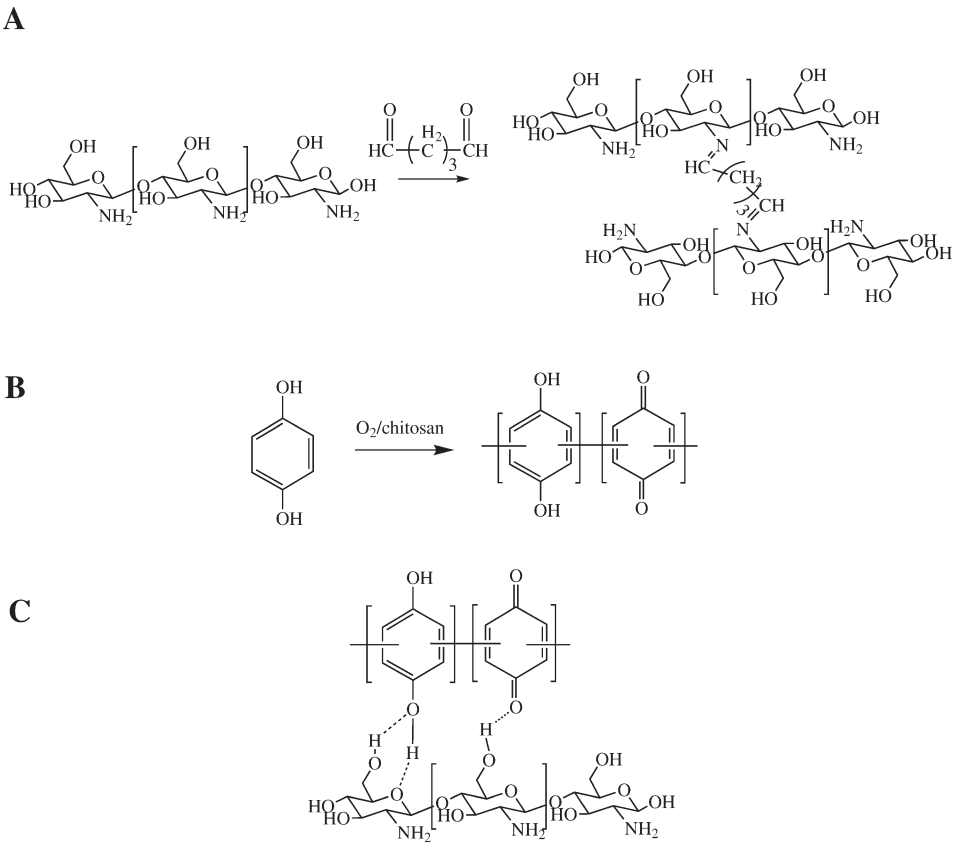

Scheme 2. (A) Spontaneous Schiff's base reaction between chitosan and glutaraldehyde. (B) The chemical reaction of oxidative polymerization of HQ. (C) The hydrogen bonding between PHQ and chitosan.

as the film continues to grow. The RMS (root mean square) roughness of the films were calculated to be 6.61, 6.47, 6.12, and 2.98 nm, for 10, 15, 20, and 25-layer films, respectively, indicating the film becomes smoother with increasing layer number. To measure the film thickness, the film was partially scratched with a razor blade.[39] The scratched area was scanned and the film thickness was calculated from the cross sectional analysis of the images. Figure 3 plots the film thickness as a function of layer number. Again a linear relationship was

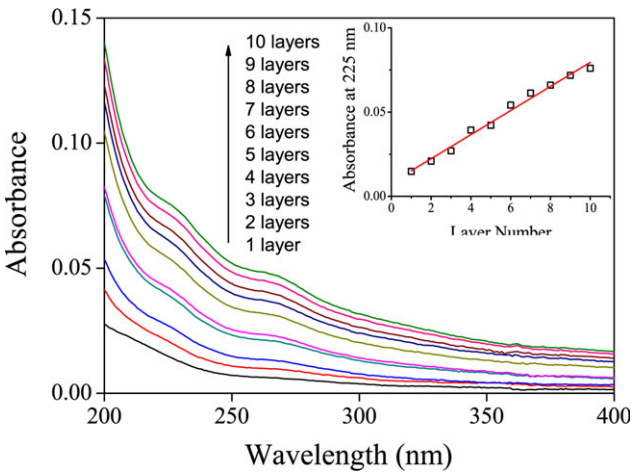

Figure 1. UV–vis spectra of LBL chitosan films with various layer numbers. Inset: absorbance at 225 nm as a function of layer number. [Color figure can be viewed in the online issue, which is available at wileyonlinelibrary.com.]

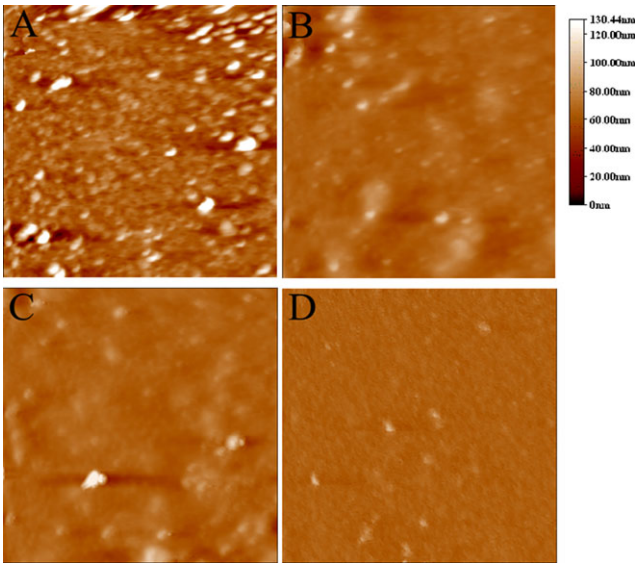

Figure 2. AFM images (10 μm × 10 μm) of single-component LBL films of chitosan. The films were fabricated on silicon wafer. The layer numbers are 10(A), 15(B), 20(C) and 25(D), respectively. [Color figure can be viewed in the online issue, which is available at wileyonlinelibrary.com.]

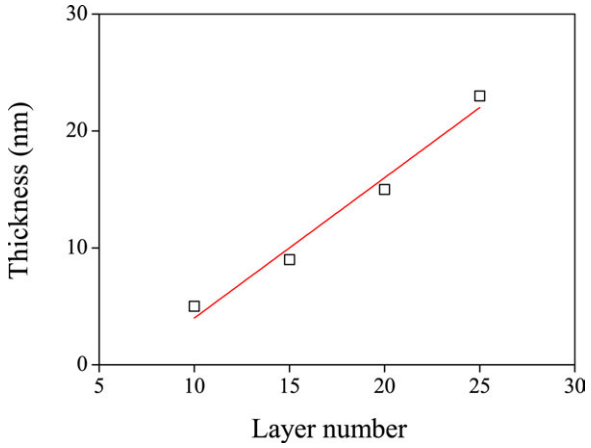

Figure 3. Thickness of the single-component chitosan LBL films measured by AFM as a function of layer number. [Color figure can be viewed in the online issue, which is available at wileyonlinelibrary.com.]

observed, confirming a linear growth for the glutaraldehyde-mediated film build-up. The average thickness increase per dipping cycle is less than 1 nm. A small thickness increase per dipping cycle will allow for more accurate control over the film thickness.

Template Polymerization of HQ in LBL Film

PHQ is usually synthesized by oxidative polymerization of HQ or *p*-benzoquinone in alkali solutions.[40,41] To obtain products with well-defined structures, sophisticated biochemical process[10] and organometallic polycondensation process[42] were also developed. Recently we found that the oxidative polymerization of HQ in acidic solutions, instead of in alkali solutions, can be achieved using chitosan as template.[9] Here we check if the template polymerization of HQ can take place in the chitosan films. For this purpose, single-component chitosan films were soaked in HQ solution. The reaction was monitored by measurement of the absorption spectra of the film at proper time intervals. As shown in Figure 4(A), at the beginning the absorption of the film in the visible range is negligible; however, it increases gradually with time. A broad peak appears at ~440 nm after 14 h immersion and its intensity continues to increase with time. We previously observed similar spectra changes from mixed solutions of chitosan/HQ under similar conditions, which have been attributed to the formation of PHQ as a result of the oxidative polymerization of HQ.[9] Here the evolution of the film spectra should also indicate the formation of PHQ in the film.

Changes in FTIR spectra also confirm the formation PHQ in the chitosan film. Figure 5 shows the FTIR spectra of a chitosan film before and after treatment in HQ solution. Compared with the spectra of the pristine film, several new absorption bands were detected. All these bands can be assigned to the new-formed PHQ. In particular, the peaks at 1595, 1508, and 1458 cm^{-1} can be assigned to the vibrations of aromatic rings and C[dbond]C bonds in the backbone of PHQ. The peak at 1206 cm^{-1} can be assigned to the phenolic OH groups. Peaks at 813 and 753 cm^{-1} can be assigned to the out-of-plane vibrations of the C[sbond]H bonds of the aromatic rings.[43–45]

The formation of PHQ also changes the morphology of the film as revealed by AFM study. As shown in Figure 6, the pristine chitosan film is relatively smooth with a RMS roughness of ~6.61 nm. After the reaction the film becomes much rougher. The RMS roughness increased to ~13.5 nm. The increased roughness may be explained by the increased heterogeneity of the film as a result of the introduction of a new component,

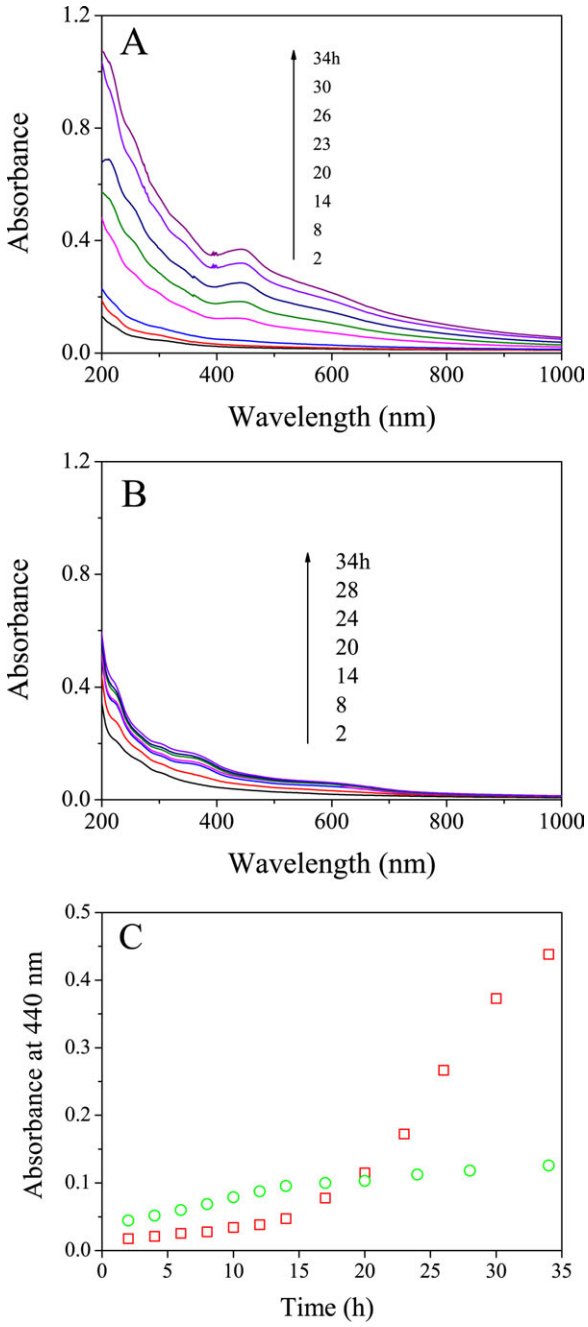

Figure 4. UV–vis spectra of a 10 layer chitosan film (A) and PEI film (B) after soaking in HQ solution (in 0.1*M* HAc) for various periods of time. [HQ] = 4.0 wt %. T = 60°C. The treatment time was shown in the figure. (C) Absorbance of the chitosan film(□) or PEI film (○) at 440 nm as a function of soaking time. [Color figure can be viewed in the online issue, which is available at wileyonlinelibrary.com.]

Applied Polymer SCIENCE

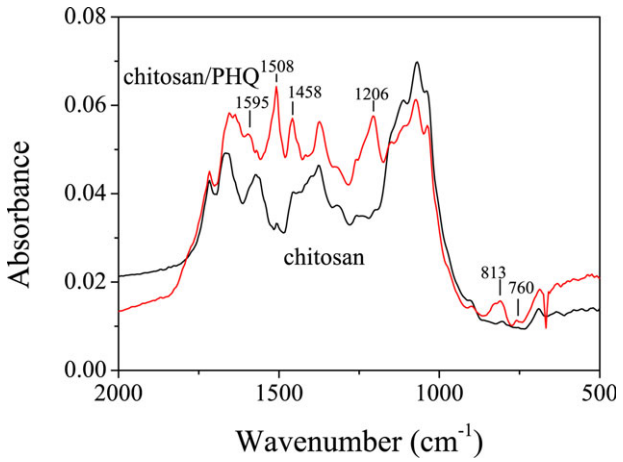

Figure 5. FTIR spectra of a chitosan LBL film and the corresponding chitosan/PHQ film. [Color figure can be viewed in the online issue, which is available at wileyonlinelibrary.com.]

PHQ. Thicknesses of a 10 layer chitosan film before and after HQ treatment were also measured. A onefold increase was found (from ~9 nm to ~20 nm after 120 h treatment). As a control, another chitosan film was treated under the same conditions but in the absence of HQ. No change in film thickness was found, suggesting the increased film thickness after HQ treatment should be attributed to the formation of PHQ.

All these results indicate the successful introduction of PHQ, which is a result of the *in situ* oxidative polymerization of HQ in the chitosan film. As mentioned above, the oxidative polymerization of HQ can take place in acidic solutions in the presence of chitosan.[9] In that case, oxygen and chitosan act as oxidant and template for the polymerization of HQ, respectively. To study the role of oxygen in the present case, a control experiment was carried out, in which the HQ solution was bubbled with nitrogen to remove oxygen. No detectable change in the UV–vis and IR spectra of the chitosan films was found, indicating the oxidative polymerization of HQ can not process in the absence of oxygen. These results suggest oxygen also acts as oxidant for the polymerization of HQ in the chitosan films.

To study the role of chitosan, control experiments were carried out in which single-component PEI films were used instead of chitosan films. The PEI films were fabricated also via the glutaraldehyde-mediated assembly. As shown in Figure 4(B), when a PEI film was soaked in HQ solution, some changes in its UV–vis spectra were observed too. However the absorption increase was much lower compared with the chitosan film [Figure 4(C)], indicating that the oxidative polymerization of HQ occurs at a much slower rate. Actually the increased absorbance of the film may be attributed to the adsorption of some negatively charged species, which are products of the oxidation of HQ by oxygen in the solution, onto the positively charged film. The absorption increase slows down after ~15 h reaction may suggest that the film surface is almost completely covered at this point. In addition, no absorption band appears at ~440 nm in the spectra of PEI film, suggesting that there was no such PHQ structure formed. Figure 4(C) also show that the reaction in chitosan film increases with time, which may be explained by a decreased crosslinking density of film, which allows the film to swell to a larger degree and hence an increase reaction rate. The film thickness change was also examined by AFM. After the HQ treatment, the thickness of a 10 layer PEI film increases slightly from ~30 to ~33 nm, corresponding to ~10% increase. As mentioned above, the thickness increase is one fold in the case of chitosan film. The much faster reaction in chitosan film than in PEI film suggests that chitosan acts as template for the polymerization of HQ. We speculate that because of its configuration, chitosan can interact with PHQ more effectively via hydrogen bonding as illustrated in Scheme 2(C), and thus making it a good template for the polymerization of HQ. PHQ should form not only on the surface of the film, but also in the interior of the film, as illustrated in Scheme 1, because both the chitosan chains on the surface and in the interior can act as template for the oxidative polymerization of HQ.

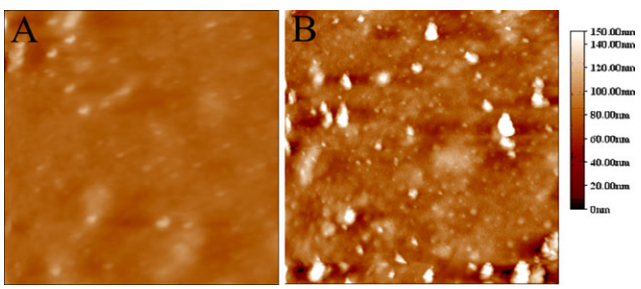

Figure 6. AFM images (10 μm × 10 μm) of 15 layers single-component chitosan LBL films before (A) and after (B) treatment in 4.0 wt % HQ (in 0.1*M* HAc) at 37°C for 5 days. [Color figure can be viewed in the online issue, which is available at wileyonlinelibrary.com.]

Electrochemical Properties of Chitosan/PHQ Film

To study the electrochemical properties of the LBL films, they were fabricated on ITO glass. The cyclic voltammograms were measured in 0.1*M* phosphate buffer (pH = 7.3). As shown in Figure 7, in the CV chart of the pristine chitosan film, within

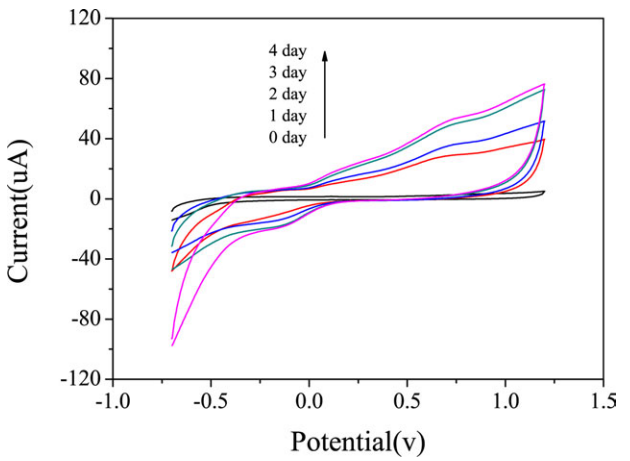

Figure 7. Cyclic voltammograms of a 10-layer single-component chitosan LBL film after treatment in HQ solution (in 0.1*M* HAc). The treatment time is 0, 1, 2, 3, and 4 days, respectively. [HQ] = 4.0 wt %. T = 60°C. [Color figure can be viewed in the online issue, which is available at wileyonlinelibrary.com.]

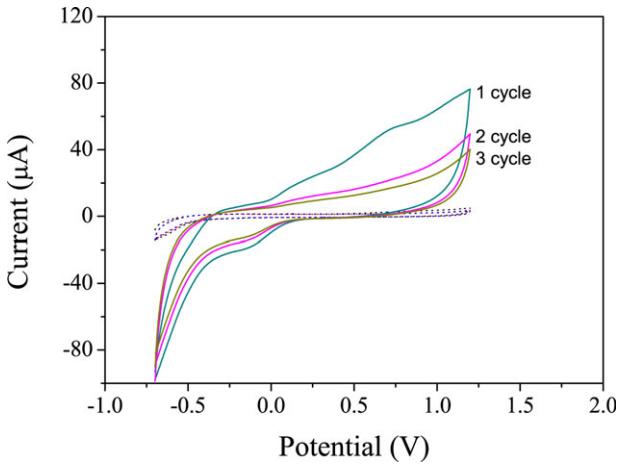

Figure 8. Cyclic voltammograms of a single-component chitosan LBL film (dotted line) and a chitosan/PHQ film (solid line) fabricated on ITO glass in 0.1*M* pH 7.3 phosphate buffer. The sweeping velocity is 0.1 V s^{-1}. Reference electrode: Ag/AgCl. [Color figure can be viewed in the online issue, which is available at wileyonlinelibrary.com.]

the scanning potential range both anodic and cathodic currents are extremely low, indicating the film is not redox-active. With the introduction of PHQ, however, both currents increase significantly, indicating the film becomes redox-active. In addition, both currents increase with increasing treatment time in HQ solution, suggesting the more PHQ generates in the film, the more redox-active species are available for the electrochemical oxidation and reduction at the electrode surface.

Compared with the CV chart of the chitosan/PHQ hydrogel we prepared previously,[9] both similarities and divergences were observed. The chitosan/PHQ hydrogel shows two well-defined oxidation peaks and two reduction peaks. Similarly, the chitosan/PHQ film shows two oxidation peaks at 0.21 and 0.75 V, respectively, but only one reduction peak at −0.15 V (vs Ag/AgCl). In addition, the two oxidation peaks are not well-defined. The similarities should originate from the fact that both materials are essentially hydrogels composed of the same components. Previously similar electrochemical properties were reported for PHQ synthesized by organometallic polycondensation of dihaloaromatic compounds.[42] The difference may originate from the confinement of the crosslinked film on PHQ species, which makes the redox reaction of PHQ less reversible.

Figure 8 shows that both oxidation and reduction currents decrease significantly when repeated scanning the chitosan/PHQ film. Previously Yamamoto et al.[42] showed that repeated scanning gave almost the same CV curve when PHQ is dissolved in DMF; however, CV curve of a cast film strongly depended on the repeating number of scanning, because the film provides hydrophobic circumstances for the quinone unit. We previously observed that repeated scanning does not change the CV curve of chitosan/PHQ hydrogel, because the low crosslinking density of the hydrogel allows for the redox-active PHQ diffuse to and away from the electrode surface, therefore, the hydrogel behaviors more like a real solution.[42] Here the chitosan film is covalently crosslinked by glutaraldehyde, the diffuse of PHQ species should be difficult, therefore it behaviors more like a real solid film.

CONCLUSIONS

We synthesized redox-active chitosan/PHQ thin films which is a chitosan hydrogel matrix trapped with redox-active PHQ. Single-component LBL films were first fabricated by the glutaraldehyde-mediated assembly of chitosan. PHQ was then introduced by the *in situ* oxidative polymerization of HQ in the film. In this reaction, oxygen acts as oxidant and chitosan as template. The template effect of chitosan was confirmed by the accelerated reaction in chitosan film compared with that in PEI film. Preliminary electrochemical test indicates that the resultant film is redox-active. We expect that the new redox films will find application in the design of new amperometric biosensors.

ACKNOWLEDGMENTS

YG thanks financial support from National Natural Science Foundation of China (Grants No. 20974049 and 21274068), and Tianjin Committee of Science and Technology (10JCYBJC02000). YZ thanks financial support for this work from the Ministry of Science and Technology of China (Grant No.: 2007DFA50760) and Program for New Century Excellent Talents in University (NCET-11-0264).

REFERENCES

1. Heller, A. *Curr. Opin. Chem. Biol.* **2006**, *10*, 664.
2. Tamaki, T.; Ito, T.; Yamaguchi, T. *J. Phys. Chem. B* **2007**, *111*, 10312.
3. Boztas, A. O.; Guiseppi-Elie, A. *Biomacromolecules* **2009**, *10*, 2135.
4. Liu, H. M.; Liu, C. X.; Jiang, L. Y.; Liu, J.; Yang, Q. D.; Guo, Z. H.; Cai, X. X. *Electroanalysis* **2008**, *20*, 170.
5. Mano, N.; Yoo, J. E.; Tarver, J.; Loo, Y. L.; Heller, A. *J. Am. Chem. Soc.* **2007**, *129*, 7006.
6. Brahim, S.; Guiseppi-Elie, A. *Electroanalysis* **2005**, *17*, 556.
7. Merchant, S. A.; Glatzhofer, D. T.; Schmidtke, D. W. *Langmuir* **2007**, *23*, 11295.
8. Mano, N.; Mao, F.; Heller, A. *Chembiochem* **2004**, *5*, 1703.
9. He, J.; Zhang, A.; Zhang, Y.; Guan, Y. *Macromolecules* **2011**, *44*, 2245.
10. Wang, P.; Martin, B. D.; Parida, S.; Rethwisch, D. G.; Dordick, J. S. *J. Am. Chem. Soc.* **1995**, *117*, 12885.
11. Kumar, M.; Muzzarelli, R.; Muzzarelli, C.; Sashiwa, H.; Domb, A. J. *Chem. Rev.* **2004**, *104*, 6017.
12. Decher, G. *Science* **1997**, *277*, 1232.
13. Tang, Z. Y.; Wang, Y.; Podsiadlo, P.; Kotov, N. A. *Adv. Mater.* **2006**, *18*, 3203.
14. Tong, W. J.; Gao, C. Y. *J. Mater. Chem.* **2008**, *18*, 3799.
15. Zhang, X.; Chen, H.; Zhang, H. Y. *Chem. Commun.* **2007**, 1395.
16. Lutkenhaus, J. L.; Hammond, P. T. *Soft Matter* **2007**, *3*, 804.
17. Bergbreiter, D. E.; Liao, K. *Soft Matter* **2009**, *5*, 23.

18. Such, G. K.; Johnston, A.; Caruso, F. *Chem. Soc. Rev.* **2011**, *40*, 19.
19. Kozlovskaya, V.; Kharlampieva, E.; Erel, I.; Sukhishvili, S. A. *Soft Matter* **2009**, *5*, 4077.
20. Ding, Z. B.; Guan, Y.; Zhang, Y. J.; Zhu, X. X. *Polymer* **2009**, *50*, 4205.
21. Zhang, X.; Guan, Y.; Zhang, Y. *Biomacromolecules* **2012**, *13*, 92.
22. Joly, S.; Kane, R.; Radzilowski, L.; Wang, T.; Wu, A.; Cohen, R. E.; Thomas, E. L.; Rubner, M. F. *Langmuir* **2000**, *16*, 1354.
23. Wang, T. C.; Rubner, M. F.; Cohen, R. E. *Langmuir* **2002**, *18*, 3370.
24. Xiao, S. L.; Wu, S. Q.; Shen, M. W.; Guo, R.; Huang, Q. G.; Wang, S. Y.; Shi, X. Y. *ACS Appl. Mater. Interf.* **2009**, *1*, 2848.
25. Machado, G.; Beppu, M. M.; Feil, A. F.; Figueroa, C. A.; Correia, R. R. B.; Teixeira, S. R. *J. Phys. Chem. C* **2009**, *113*, 19005.
26. Zhang, W.; Zhang, A.; Guan, Y.; Zhang, Y.; Zhu, X. X. *J. Mater. Chem.* **2011**, *21*, 548.
27. Xiong, H. M.; Cheng, M. H.; Zhou, Z.; Zhang, X.; Shen, J. C. *Adv. Mater.* **1998**, *10*, 529.
28. Dante, S.; Hou, Z.; Risbud, S.; Stroeve, P. *Langmuir* **1999**, *15*, 2176.
29. Kidambi, S.; Dai, J.; Li, J.; Bruening, M. L. *J. Am. Chem. Soc.* **2004**, *126*, 2658.
30. Dai, J. H.; Bruening, M. L. *Nano Lett.* **2002**, *2*, 497.
31. Lee, D.; Cohen, R. E.; Rubner, M. F. *Langmuir* **2005**, *21*, 9651.
32. Shi, X. Y.; Briseno, A. L.; Sanedrin, R. J.; Zhou, F. M. *Macromolecules* **2003**, *36*, 4093.
33. Yang, X. M.; Dai, T. Y.; Wei, M.; Lu, Y. *Polymer* **2006**, *47*, 4596.
34. Ghan, R.; Shutava, T.; Patel, A.; John, V. T.; Lvov, Y. *Macromolecules* **2004**, *37*, 4519.
35. Allan, G. G.; Peyron, M. *Carbohydr. Res.* **1995**, *277*, 257.
36. Manna, U.; Dhar, J.; Nayak, R.; Patil, S. *Chem. Commun.* **2010**, *46*, 2250.
37. Zhang, L.; Shen, Y. H.; Xie, A. J.; Li, S. K.; Wang, C. *J. Mater. Chem.* **2008**, *18*, 1196.
38. Zhang, Y. J.; Guan, Y.; Zhou, S. Q. *Biomacromolecules* **2005**, *6*, 2365.
39. McAloney, R. A.; Sinyor, M.; Dudnik, V.; Goh, M. C. *Langmuir* **2001**, *17*, 6655.
40. Cataldo, F. *Polym. Int.* **1998**, *46*, 263.
41. Furlani, A.; Russo, M. V.; Cataldo, F. *Synth. Metals* **1989**, *29*, 507.
42. Yamamoto, T.; Kimura, T. *Macromolecules* **1998**, *31*, 2683.
43. Sadykh-Zade, S. I.; Ragimov, A. V.; Suleimanova, S. S.; Liogon'Kii, B. I. *Vysokomolekulyarnye Soedineniya Seriya A* **1972**, *14*, 1248.
44. Berlin, A. A.; Ragimov, A. V.; Sadykh-Zade, S. I.; Gadzhieva, T. A.; Takhmazov, B. M. *Vysokomolekulyarnye Soedineniya Seriya A* **1975**, *17*, 111.
45. Ragimov, A. V.; Mamedov, B. A.; Liogon'Kii, B. I. *Vysokomolekulyarnye Soedineniya Seriya A* **1977**, *19*, 2538.